Acta Mechanica 147, 73–86 (2001)

ACTA MECHANICA

De-icing by slot injection

A. D. Fitt and **M. P. Pope,** Southampton, United Kingdom

(Received January 21, 2000)

Summary. We consider the removal of ice from a plate in a cold cross flow by injection of hot fluid through a slot in the plate. De-icing of this sort is required in a number of diverse industrial scenarios, and is particularly relevant to the aviation industry, where the presence of ice on aircraft wings is a major safety hazard. Thin aerofoil theory is used to determine the flow above the injected fluid layer, and this is coupled to flow and energy equations in the injected layer and the ice. The key non-dimensional parameters and ratios in the problem are identified. The result is a nonlinear singular integro-differential equation which is coupled to a convection/diffusion equation and a Stefan condition. Some special cases are discussed and some asymptotic limits are identified. The problem is then solved numerically, and results for a number of different cases are presented

1 Introduction

In this study we wish to consider the de-icing, by slot injection of warm fluid, of iced surfaces in a cross flow. Though the model that we shall discuss is relevant in a number of diverse industrial scenarios, its most important and easily-understood application is the removal of ice accumulations from aircraft wings. Ice causes the effective shape of an aircraft wing to alter, increases the drag and decreases the lift (see, for example [1]). The presence of ice on aircraft wings is potentially extremely hazardous. References [2] and [3] both report aircraft crashes that were directly attributable to ice that had accumulated on the aircraft's wings during flight.

The methods by which ice accumulation may be tackled fall broadly into two categories: "anti-icing", where the aim is to prevent ice accumulation from ever happening, and "de-icing", which normally takes place during flight.

The commonest method of anti-icing involves spraying the aircraft with de-icing chemicals prior to take-off. The most common de-icing agents are propylene glycol or ethylene glycol ([2]). Unfortunately, these liquids are not effective for more than about 30 minutes of flight time, after which re-icing becomes a danger. More advanced chemicals are currently being developed which may adhere to the aircraft for longer (see, for example [2]).

The main methods of de-icing are listed in [3]. These include (i) use of freezing piont depressants, (ii) surface deformation and (iii) thermal melting. To use freezing point depressants an arrangement is set up whereby the leading edges of the wings contain slots, through which ethylene glycol is expelled during flight. The glycol de-ices the aft parts of the wing by flowing over the ice layer. Experimental testing of this method [4] showed it to be an effective method of de-icing. The main drawback of this system is that the required glycol must be stored on board, thus increasing the weight of the aircraft. In practice pilots normally control the glycol release by observing the aircraft's wings to detect ice accumulation ([2]), though

optical sensors are currently being developed in an attempt to automate the process and optimize glycol consumption. In surface deformation de-icing the general idea is to crack the ice layer by directly deforming the wing. The ice is then carried away by the outer flow. One popular method uses pneumatic "boots" which consist of inflatable bladders that are fixed to the wing and instantaneously inflated when required during flight. It is suggested in [5] that this method is most commonly used on turbo-propeller driven commercial aircraft because such engines do not generate sufficient heat to effectively de-ice the external surfaces. Another successful surface deformation method is electromagnetic impulse de-icing (EIDI) where parts of the outer surface of the aircraft are deformed by passing an electrical current through a coil located just underneath the aircraft's skin. The opposing magnetic fields in the coil and the shell repel each other and the surface is deformed for a fraction of a second. Although EIDI is effective, the repeated rapid deformations involved may lead to wing fatigue; the electromagnetic energy produced by the coil may also interfere with the avionics of the aircraft.

Thermal melting of ice layers may be achieved by three main methods: (a) the use of electrothermal heaters situated on the aircraft's wings, (b) the passing of hot air under the skin of the aircraft, and (c) slot injection of hot gas on to the wing surface. Electrothermal heaters require electrical energy in order to produce heat and thus increase the power consumption of the aircraft. Since such heaters do not normally cover the entire wing, ice is free to form on other parts of the wing. On modern commercial airliners, electrical heating is used only for de-icing external probes and sensors and for the flight deck windscreens. Reference [5] states that passing hot air under the skin of the aircraft (normally known as "hot wing" de-icing) is the most popular de-icing method used on modern jet aircraft; most modern jet engines produce sufficient heat to successfully de-ice the entire surface of both wings.

This study concerns the method of de-icing by slot injection. Here, hot air is expelled through slots in the leading edge of the wing and gradually removes the layer of ice from above (and not from below as in (a) and (b) above). This eliminates problems associated with the possibility of large pieces of ice detaching from the wing and travelling downstream. Slot injection de-icing enjoys the additional advantage that because hot air from the engines may be used, de-icing my be activated for the duration of the flight. The method may thus be used for both de-icing and anti-icing.

2 Mathematical analysis of slot injection de-icing

The groundwork for the development presented below was carried out in [6] and [7], where isothermal slot injection into a high Reynolds number cross flow was studied. A further study [8] considered film-cooling effectiveness for the injection of a cold fluid into a cross flow. All of these studies however considered only steady flow; the problem discussed below is unsteady. We consider a two dimensional irrotational inviscid incompressible cross flow whose density is ρ and whose pressure, temperature and velocity far upstream of a slot of width L are p_∞, θ_∞ and $U_\infty \mathbf{e}_x$, respectively, where $\mathbf{e}_x$ is a unit vector in the x-direction. Immediately downstream of the slot (whose upstream edge is assumed to be at the origin) is an ice layer whose height is denoted by $B(x, t)$. The general arrangement is shown in Fig. 1.

Deep within the injection slot, we assume that the injected fluid has temperature θ_i. Its pressure must be carefully maintained so that exactly the right amount issues from the slot: if the slot pressure p_s is too high then the hot fluid will spurt vertically upwards and be "lost" in the outer flow, but if it is too low then insufficient melting will take place. We therefore

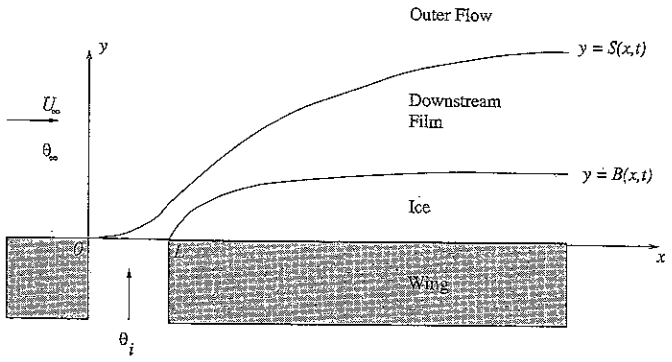

Fig. 1. Schematic diagram of the de-icing problem

assume that

$$p_s = p_\infty + \frac{1}{2}\rho U_\infty^2 \epsilon^2 , \tag{1}$$

thereby defining ϵ, the key small parameter in the problem. Since the disturbance produced in the cross flow is small, classical thin areofoil theory will be applicable. As in [9] and [6], we assume that the boundary layer on the flat plate is "blown off" by the injection and forms a shear layer that seperates the injected and outer flows. Thin aerofoil theory now dictates that the injected flow (whose boundary is denoted by $S(x,t)$) will form a layer of thickness $O(\epsilon^2 L)$. The horizontal speed of the flow in the injected layer is thus $O(\epsilon U_\infty)$, and the mass flow from the slot is $O(\epsilon^3 \rho U_\infty L)$.

We now analyse the flow in the injected fluid downstream of the slot (the "film" region). We nondimensionalise by setting $x = Lx^*$, $y = \epsilon^2 L y^*$, $S = \epsilon^2 L S^*$, $B = \epsilon^2 L B^*$ and $\psi = \epsilon^3 L U_\infty \psi^*$ where ψ denotes the stream function of the injected flow and a star is used to denote nondimensional variables. To leading order the governing equation

$$\psi_{xx} + \psi_{yy} = 0$$

becomes

$$\psi^*_{y^*y^*} = 0 ,$$

and thus, defining the nondimensional mass flow M^* by $M = \rho L U_\infty \epsilon^3 M^*$, we have (since $\psi^* = 0$ on $y^* = B^*$ and $\psi^* = M^*$ on $\psi^* = S^*$)

$$\psi^* = \frac{M^*(y^* - B^*)}{(S^* - B^*)} \tag{2}$$

The nondimensional horizontal velocity u^* in the film is thus

$$u^* = \frac{M^*}{S^* - B^*} \tag{3}$$

Bernoulli's equation may now be applied in the film region to determine the pressure. We nondimensionalize the pressure in the film region by setting $p_f = \rho U_\infty^2 p_f^*$. Making the important assumption that the orders of magnitude that apply deep within the the injection slot are appropriate all the way up to the top of the slot, we now have

$$p_f^* = \frac{p_\infty}{\rho U_\infty^2} + \frac{1}{2}\epsilon^2 \quad (0 \le x^* \le 1) , \tag{4}$$

and, using (3),

$$p_f^* = \frac{p_\infty}{\rho U_\infty^2} + \frac{1}{2}\epsilon^2\left(1 - \frac{M^{*2}}{(S^* - B^*)^2}\right) \quad (1 \le x^*) \tag{5}$$

Now that the pressure is known in the film region, we must ensure that it is continuous across $y^* = S^*(x^*, t^*)$. In the cross flow, the stream function ψ_o may be written

$$\psi_o(x, y) = U_\infty y + \frac{\epsilon^2 U_\infty}{\pi}\int_0^\infty g(\eta, t)\tan^{-1}\left(\frac{y}{x - \eta}\right)d\eta, \tag{6}$$

where $g(x,t)$ is the (as yet unknown) nondimensional source distribution strength which represents the perturbation to the flow caused by the injected layer. Since $y = S(x,t)$ must be a streamline of the flow, we have $(D/Dt)(y - S(x,t)) = 0$ and thus, on $y = S(x,t)$,

$$S_t + uS_x = v \tag{7}$$

We now nondimensionalize in the outer flow by setting $x = L\hat{x}$, $y = L\hat{y}$, $S = \epsilon^2 L\hat{S}$, $\psi_o = LU_\infty\hat{\psi}_o$, $u = U_\infty\hat{u}$, $v = \epsilon^2 U_\infty\hat{v}$, $p_o = \rho U_\infty^2\hat{p}_o$ and $t = \tau\hat{t}$. The boundary condition (7) asserts that

$$\left(\frac{L}{U_\infty\tau}\right)\hat{S}_{\hat{t}} + \hat{u}\hat{S}_{\hat{x}} = \hat{v} \tag{8}$$

on $\hat{y} = \epsilon^2\hat{S}(\hat{x}, \hat{t})$. Standard thin-aerofoil theory applies, and (8) is therefore imposed to leading order on $\hat{y} = 0$. Since we wish to identify various parameter regimes and time scales, we do not, as yet, identify the parameter τ, but merely assume that $L/U_\infty\tau \ll 1$. (When $L/U_\infty\tau = O(1)$, an unsteady, fully coupled formulation of the problem applies; we do not pursue this further here, however.) In this case, consideration of the behaviour of (6) in the limit as $\hat{y} \to 0$ gives that, to leading order, $g(x,t) = S_x(x,t)$. The nondimensional pressure in the outer flow on $\hat{y} = 0$ may now be determined using Bernoulli's equation. We find that

$$\hat{p}_o = \frac{p_\infty}{\rho U_\infty^2} - \frac{\epsilon^2}{\pi}\int_0^\infty \frac{\hat{S}_{\hat{\eta}}(\hat{\eta}, \hat{t})}{\hat{x} - \hat{\eta}}\,d\hat{\eta} \tag{9}$$

We now match (9) to (4) and (5). This gives

$$\frac{1}{\pi}\int_0^\infty \frac{S^*_{\eta^*}(\eta^*, t^*)}{x^* - \eta^*}\,d\eta^* = \begin{cases} -\dfrac{1}{2} & 0 \le x^* \le 1 \\ -\dfrac{1}{2} + \dfrac{M^{*2}}{2(S^* - B^*)^2} & x^* \ge 1 \end{cases} \tag{10}$$

Finally, we require boundary conditions for (10). Since the total pressure in the outer flow is given by $p_{t\infty} = p_\infty + \rho U_\infty^2/2$ and the total pressure in the slot is $p_\infty + \frac{1}{2}\rho U^2{}_\infty\epsilon^2 + O(\epsilon^6)$, the flow must separate tangentially from the upstream edge of the slot. Thus

$$S^*(0, t^*) = S^*_{x^*}(0, t^*) = 0$$

3 Energy equation

To close the model, a second equation must be derived that relates $S^*(x^*,t^*)$ to $B^*(x^*,t^*)$ This equation must account for the heat transfer that takes place in the film layer and the change of phase that occurs when the ice melts. We assume that the melting point of the ice is given by θ_f, and that the wall at $y=0$ is maintained at a constant temperature θ_w In the film layer, the energy equation is

$$\rho_f c_{pf}(\theta_t^- + (\mathbf{q}_f \nabla)\theta^-) = k_f(\theta_{xx}^- + \theta_{yy}^-)\,, \tag{11}$$

where θ^- denotes temperature, $\boldsymbol{q}_f$, denotes the film velocity and ρ_f, c_{pf} and k_f are respectively the density, specific heat at constant pressure and thermal conductivity of the injected fluid. We now nondimensionalize (11) according to $x = Lx^*$, $y = \epsilon^2 Ly^*$, $S = \epsilon^2 LS^*$, $B = \epsilon^2 LB^*$, $u = \epsilon U_\infty u^*$, $v = \epsilon^3 U_\infty v^*$, $t = \tau t^*$ and $\theta = \theta_f + \theta^{*-}(\theta_i - \theta_f)$. This gives

$$\frac{\epsilon^5 L U_\infty \rho_f c_{pf}}{k_f}\left(\left(\frac{L}{\epsilon U_\infty \tau}\right)\theta_{t^*}^{*-} + u^*\theta_{x^*}^{*-} + v^*\theta_{y^*}^{*-}\right) = \epsilon^4\theta_{x^*x^*}^{*-} + \theta_{y^*y^*}^{*-} \tag{12}$$

In the ice layer, the energy equation for the ice temperature θ^{*+} is similar to (11), but there is no convection Using the same nondimensionalisation as for the film region, but denoting temperature by θ^{*+} and using a subscript i to denote the thermal properties of the ice, we have

$$\frac{\epsilon^4 L^2 \rho_i c_{pi}}{k_i \tau}\,\theta_{t^*}^{*+} = \epsilon^4\theta_{x^*x^*}^{*+} + \theta_{y^*y^*}^{*+} \tag{13}$$

Clearly at this juncture there are many different problems that we could consider; however we shall now fix our attention on a specific parameter regime As we have already explained, we have assumed that the wall at $y=0$ is maintained at a given temperature θ_w Although we shall continue to assume this, the model is hardly changed at all if we alter this boundary condition to correspond to a given (possibly non-constant) wall temperature, a given heat flux, or Newton cooling Up to now have assumed only that the timescale τ satisfies $L/U_\infty\tau \ll 1$; we shall now be more specific and choose $\tau = L/(U_\infty\epsilon^2)$ since, as we shall see, this turns out to be the most interesting case. Let us now consider (12) We find that, for $\epsilon \ll 1$, to leading order we have

$$\Gamma^*[u^*\theta_{x^*}^{*-} + v^*\theta_{y^*}^{*-}] = \theta_{y^*y^*}^{*-}\,, \tag{14}$$

where

$$\Gamma^* = \frac{\epsilon^5 L U_\infty \rho_f c_{pf}}{k_f}$$

The first crucial nondimensional parameter Γ^* is thus identified Clearly if $\Gamma^* \gg 1$ the downstream heat transfer is convention-dominated, and the details of the melting of the ice are determined by a boundary layer On the other hand, if $\Gamma^* \ll 1$ then diffusion dominates. Although in this case the temperature may be completely determined and is simply linear in y^*, we do not pursue this further as clearly the melting is negligible except for a small "entry region" near to $x^* = 1$ and the de-icing process cannot function efficiently When $\Gamma^* = O(1)$ effective de-icing occurs over a number of slot widths downstream of injection This is the most interesting case, and the one that will now be analyzed

We may now reconsider (13) To leading order, we find that

$$\frac{\epsilon^6 L U_\infty \rho_i c_{pi}}{k_i}\,\theta^{*-}_{t^*} = \theta^{*-}_{y^*y^*} \tag{15}$$

The key nondimensional parameter for this equation may therefore be written as $\epsilon\Gamma^* K_i/K_f$, where K_i and K_f are the thermal diffusivities of the ice and the injected fluid, respectively. According to standard sources (see, for example [10]) the thermal diffusivities of ice and air are about $1.5\times10^{-6}\mathrm{m}^2/\mathrm{sec}$ and $6\times10^{-6}\mathrm{m}^2/\mathrm{sec}$, respectively; since $\epsilon \ll 1$ it is therefore clear that to lowest order (15) becomes

$$\theta^{*+}_{y^*y^*} = 0\,,$$

and thus

$$\theta^{*+} = \left(1-\frac{y^*}{B^*}\right)\left(\frac{\theta_w-\theta_f}{\theta_i-\theta_f}\right). \tag{16}$$

The melting of the ice is governed by a standard Stefan condition. To leading order, we have (in dimensional form)

$$[k\theta_y]^-_+ = -\rho_i L_H B_t\,, \tag{17}$$

where the square brackets denote the jump in the enclosed quantity, and L_H is the latent heat of melting of the ice. In nondimensional form, (17) becomes

$$\theta^{*-}_{y^*} - \frac{k_i}{k_f}\,\theta^{*+}_{y^*} = -\lambda^* B^*_{t^*} \tag{18}$$

on $y^* = B^*(x^*,t^*)$, where the key nondimensional parameter λ^* is given by

$$\lambda^* = \frac{\rho_i L_H \epsilon^6 L U_\infty}{k_f(\theta_i-\theta_f)}$$

As far as the physical interpretation of λ^* is concerned, we note that we require λ^* to be O(1) if the de-icing process is to be nontrivial, for if $\lambda^* \ll 1$ then the ice layer is removed immediately, while if $\lambda^* \gg 1$ the latent heat of the ice is so high that the ice layer can never be melted. (We also assume that the injected fluid is not hot enough to melt the wing; if the ice layer completely melts so that $B^* = 0$ we therefore replace (18) by $B^*_{t^*} = 0$.)

We now have enough information to close the problem. We use (2) in (14) and (16) in (18) to yield

$$\Gamma^*[\psi^*_{y^*}\theta^{*-}_{x^*} - \psi^*_{x^*}\theta^{*-}_{y^*}] = \theta^{*-}_{y^*y^*}\,, \quad \psi^* = \frac{M^*(y^*-B^*)}{(S^*-B^*)} \quad (B^* \le y^* \le S^*\,,\ x^* \ge 1)\,, \tag{19}$$

$$\theta^{*-}_{y^*} + \frac{1}{B^*}\left(\frac{k_i}{k_f}\right)\left(\frac{\theta_w-\theta_f}{\theta_i-\theta_f}\right) = -\lambda^* B^*_{t^*} \quad \text{on } y^* = B^*\,, \tag{20}$$

$$\frac{1}{\pi}\int_0^\infty \frac{S^*_{\eta^*}(\eta^*,t^*)}{x^*-\eta^*}\,d\eta^* = \begin{cases} -\dfrac{1}{2} & 0 \le x^* \le 1 \\ -\dfrac{1}{2} + \dfrac{M^{*2}}{2(S^*-B^*)^2} & x^* \ge 1 \end{cases} \tag{21}$$

with

$$\theta^{*-}(1,y^*,t^*)=1\,,\quad \theta^{*-}(x^*,B^*,t^*)=0\,,\quad \theta^{*-}(x^*,S^*,t^*)=\frac{\theta_\infty-\theta_f}{\theta_i-\theta_f}\,,$$

$$S^*(0,t^*)=S^*_{x^*}(0,t^*)=0\,,$$

and $B^*(x^*,0)$ prescribed as a function of x^* We shall henceforth refer to (19)–(21) as the "De-icing equations"

4 General comments and asymptotic limits

Clearly in general it will be necessary to solve (19)–(21) numerically. Before proceeding to do this, some general comments are in order We note first that only (20) depends explicitly upon time The problem is thus quasi-steady, and the free streamline $S^*(x^*,t^*)$ responds temporally only to changes in the thickness of the ice layer We also note that the whole problem depends only on the two nondimensional parameters Γ^* and λ^* and the ratios $k_i(\theta_w-\theta_f)\,/\,k_f(\theta_i-\theta_f)$ and $(\theta_\infty-\theta_f)\,/\,(\theta_i-\theta_f)$ Under normal aviation circumstances we expect that $\theta_i>\theta_f>\theta_w>\theta_\infty$ (though other cases may occasionally be relevant), and thus $\lambda^*>0$ The second term on the left-hand side of the Stefan condition (20) thus tends to make the ice layer become thicker (For the present, we assume that the injected fluid contains sufficient water vapour for ice growth to be possible if the thermal conditions permit) Near to the injection slot, it is the first term of (20) which melts the ice, as $\theta^{*-}_{y^*}>0$ if the injected fluid is hot enough

4 1 Downstream behavior

Some further simplifications may be made far downstream of the slot. Here the cold cross flow has had enough time to influence the once-hot film flow, and the energy equation to leading order in the film becomes $\theta^{*-}_{y^*y^*}=0$ Thus

$$\theta^{*-}=\frac{A(y^*-B^*)}{S^*-B^*}\,,$$

where $A=(\theta_\infty-\theta_f)/(\theta_i-\theta_f)$, and the Stefan condition (20) becomes

$$\frac{A}{S^*-B^*}+\frac{\kappa}{B^*}=-\lambda^*B^*_{t^*}\,,$$

where

$$\kappa=\frac{k_i}{k_f}\left(\frac{\theta_w-\theta_f}{\theta_i-\theta_f}\right)$$

The streamline height S^* may now be eliminated if desired from (21) so that a single partial integro-differential equation (which must still be solved numerically) remains.

4.2 Thin ice layers

Another case in which limited analytic progress may be made occurs when the ice layer is "thin" so that $B^* \ll S^*$. In this case, the dependence of (21) on B^* is removed, and we can make use of the fact that, for $x^* \gg 1$, the asymptotic behaviour of S^* may be determined. Standard methods give

$$S^* \sim S^*_\infty - \frac{S^{*4}_\infty}{M^{*2}\pi x^*} + O(x^{*-2}\log x^*),$$

where S^*_∞ denotes the limiting value of S^* as $x^* \to \infty$. It may easily be shown that under these circumstances $\theta^{*-}_{y^*} \sim 1/S^*$ on $y^* = B^*$, and thus to leading order (20) becomes

$$-\lambda^* B^*_{t^*} B^* \sim \kappa$$

Far downstream, we therefore expect that

$$B^* \sim \sqrt{C_1 - 2\kappa t^*/\lambda^*},$$

where C_1 is a constant. Since under normal circumstances $\kappa < 0$, this gives the expected result that the ice layer grows like $\sqrt{t^*}$ far downstream of the slot and for large times.

A number of other asymptotic limits (based, for example, on large or small temperature ratios and/or thermal conductivity ratios) admit simplifications and may be considered: in most cases however the details are fairly straightforward; we do not pursue these limits further.

5 Numerical solution of the de-icing equations

In general, (19)–(21) must be solved numerically. This may be done using a simple iterative method. We start by solving the singular integro-differential equation (21) for S^*, assuming that an initial B^* is known. This also determines M^*. We then use these values of M^*, S^* and B^* in (19) and solve this convection/diffusion equation to yield θ^{*-} and thus $\theta^{*-}_{y^*}(x^*, B^*, t^*)$. A simple explicit scheme may now be used to update B^* from (20), after which the whole process may be repeated. We deal with each of these substeps in turn.

5.1 Singular integro-differential equation

The method that we use to solve the singular integro-differential equation (21) is similar to that employed in [6], save for the fact that the ice layer must be accounted for. The first step is to invert (21) and apply the boundary condition $S^*_{x^*}(0, t^*) = 0$ to obtain

$$S^*_{x^*}(x^*, t^*) = \frac{\sqrt{x^*}}{2\pi} \int_1^\infty \frac{M^{*2} d\eta^*}{[S^*(\eta^*, t^*) - B^*(\eta^*, t^*)]^2 \sqrt{\eta^*}(\eta^* - x^*)} \tag{22}$$

At this stage it is convenient to remove M^* from (22) by setting

$$S^* = M^{*2/3} T^*, \quad B^* = M^{*2/3} C^*$$

The equation may now be integrated with respect to x^* Applying the boundary condition $T^*(0,t^*)=0$ now yields

$$T(x,t)=\frac{1}{2\pi}\int_1^{\infty}\frac{1}{[T(\eta,t)-C(\eta,t)]^2}\left\{-2\sqrt{\frac{x}{\eta}}+\log\left|\frac{\sqrt{\eta}+\sqrt{x}}{\sqrt{\eta}-\sqrt{x}}\right|\right\}d\eta, \tag{23}$$

where here and henceforth the asterisks have been omitted for simplicity The form of (23) is particularly convenient from a numerical point of view as the integral is no longer a Cauchy principal value and no numerical differentiation of the unknown functions is required.

For a given time, t_m say, we now divide the range of integration $[1,\infty)$ into two regions: $[\eta_0,\eta_N]$ (with $\eta_0=1$) and $[\eta_N,\infty)$ The general idea is to use direct numerical discretization over the former interval and asymptotic estimates over the latter We divide $[\eta_0,\eta_N]$ into N equally-spaced intervals and assume that at each instant in time $T-C$ may be approximated on each sub-interval $[\eta_k,\eta_{k+1}]$, $(k=0,\quad,N-1)$ by using a piecewise linear average to give

$$2\pi T(x_i,t_m)\approx\sum_{k=0}^{N-1}\frac{1}{2}\left(\frac{1}{[T(\eta_k,t_m)-C(\eta_k,t_m)]^2}+\frac{1}{[T(\eta_{k+1},t_m)-C(\eta_{k+1},t_m)]^2}\right)$$

$$\times\int_{\eta_k}^{\eta_{k+1}}\left\{-2\sqrt{\frac{x_i}{\eta}}+\log\left|\frac{\sqrt{\eta}+\sqrt{x_i}}{\sqrt{\eta}-\sqrt{x_i}}\right|\right\}d\eta+E_{N+1} \tag{24}$$

for $i=0,\quad,N$ and where the "error" term E_{N+1} is given by

$$E_{N+1}=\int_{\eta_N}^{\infty}\frac{1}{[T(\eta,t_m)-C(\eta,t_m)]^2}\left\{-2\sqrt{\frac{x_i}{\eta}}+\log\left|\frac{\sqrt{\eta}+\sqrt{x_i}}{\sqrt{\eta}-\sqrt{x_i}}\right|\right\}d\eta \tag{25}$$

The integral in (24) may now be evaluated, and by assuming that η_N is large enough to permit the approximation of (25) we employ relaxation as in [6] to yield the numerical scheme

$$\overline{T}_{j+1}(x_i,t_m)=\frac{1}{4\pi}\sum_{k=0}^{N-1}A_{ik}([T_j(\eta_k,t_m)-C_j(\eta_k,t_m)]^{-2}+[T_j(\eta_{k+1},t_m)-C_j(\eta_{k+1},t_m)]^{-2}$$

$$+\frac{x_i}{\pi}\,Q\left(\frac{\sqrt{\eta_N}}{x_i}\right)[T_j(\eta_N,t_m)-C_j(\eta_N,t_m)]^{-2} \tag{26}$$

$$T_{j+1}(x_i,t_m)=T_j(x_i,t_m)+\phi[\overline{T}_{j+1}(x_i,t_m)-T_j(x_i,t_m)]$$

for $i=0,\quad,N$, where the relaxation parameter ϕ is chosen to be less than unity (in practice, choosing $\phi\sim 0\,1-0\,5$ usually gives good results) Here $Q(\alpha)$ is given by

$$Q(\alpha)=\alpha+\frac{1}{2}\,(1-\alpha^2)\log\left|\frac{\alpha+1}{\alpha-1}\right|, \tag{27}$$

and A_{ik} is defined by

$$A_{ik}=2\sqrt{x_i}\,(\sqrt{\eta_k}-\sqrt{\eta_{k+1}})+(\eta_{k+1}-x_i)\log\left|\frac{\sqrt{\eta_{k+1}}+\sqrt{x_i}}{\sqrt{\eta_{k+1}}-\sqrt{x_i}}\right|$$

$$-(\eta_k-x_i)\log\left|\frac{\sqrt{\eta_k}+\sqrt{x_i}}{\sqrt{\eta_k}-\sqrt{x_i}}\right| \tag{28}$$

Experience shows that the value $T(\eta_0, t_m)$ is always the slowest to converge· the scheme is therefore iterated until

$$|T_{j+1}(\eta_0, t_m) - T_j(\eta_0, t_m)| \leq \delta$$

for some prespecified tolerance δ Once convergence has taken place, values of T for $0 \leq x < 1$ may be calculated simply by using the relevant x in (24)

5.2 *Convection-diffusion equation*

To determine the temperature in the film layer, we must solve

$$M\Gamma\left[\left(\frac{1}{S-B}\right)\theta_x^- - \left(\frac{B_x(y-S) - S_x(y-B)}{(S-B)^2}\right)\theta_y^-\right] = \theta_{yy}^- \qquad (29)$$

on $x \geq 1, B(x,t) < y < S(x,t)$ with $\theta^- = 1$ at $x = 1$, $\theta^- = 0$ at $y = B$ and $\theta^- = A$ at $y = S$

In general (29) must be solved numerically, a task that may be accomplished by using a standard finite-difference method. For this particular version of de-incing however, the problem may be solved in closed form by employing a von Mises transformation. We change from independent variables (x, y) on (X, ψ) where $X = x$ and ψ is the stream function of the flow This not only transforms the partial differential equation (29) to a linear heat diffusion equation, but also, since the upper and lower boundaries of the flow are streamlines, leads to a problem that is specified on a rectangular region For a given time, the transformed boundary value problem is

$$\Gamma\theta_x{}^- = \left(\frac{M}{S(x) - B(x)}\right)\theta_{\psi\psi}^- \quad (x \geq 1,\ 0 \leq \psi \leq M)$$

with

$$\theta^-(1,\psi) = 1, \quad \theta^-(x,0) = 0, \quad \theta^-(x,M) = A$$

This may readily be solved by elementary methods to give

$$\theta^-(x,\psi) = \frac{A\psi}{M} + \sum_{n=1}^{\infty}\frac{2}{n\pi}\left[1 + (A-1)(-1)^n\right]\exp\left(-\frac{n^2\pi^2}{M^2}f(x,t)\right)\sin\left(\frac{n\pi\psi}{M}\right),$$

where

$$f(x,t) = \int_1^x \frac{M}{\Gamma(S(\xi) - B(\xi))}\,d\xi,$$

and therefore the required temperature gradient (written, for numerical purposes, in terms of T and C) is given by

$$\theta_y{}^-|_{y=B} = \frac{M^{-2/3}}{(T(x) - C(x))} \times \left[A + \sum_{n=1}^{\infty} 2[1 + (A-1)(-1)^n]\exp\left(-\frac{n^2\pi^2}{\Gamma M^{5/3}}\int_1^x \frac{d\xi}{T(\xi) - C(\xi)}\right)\right]. \qquad (30)$$

For $x > 0$ the fact that M and Γ are both order one and $T > C$ ensures that the series in (30) converges quickly. For $x = 0$ it diverges, as might be anticipated from the boundary conditions of the original boundary value problem. The physical interpretation of this is clear: if we begin the de-icing process with (for example) a layer of ice of constant thickness, then instantaneously the ice at $x = 0$ melts as the temperature is forced to jump here, and the temperature gradient is therefore infinite.

Numerically, we simply use (30) in the Stefan condition (20) and (since T and C are known only at given mesh points) calculate the necessary integrals using a simple numerical quadrature law (Simpson's rule was used in the results presented below). The series in (30) is then summed until the required accuracy is attained.

5.3 *Stefan condition*

Finally, we must update B (or, for numerical purposes, C) using (20). Some numerical experiments showed that a simple Euler method was quite sufficient to provide the required numerical accuracy, provided that a small enough time step dt was used. We write (20) as

$$C_t = -\frac{\theta_y^-|_{y=B}}{\lambda M^{2/3}} - \frac{\kappa}{C\lambda M^{4/3}}$$

and discretize this using

$$C_i^{m+1} = C_i^m - dt\left[\frac{\theta_y^-|_{y=B}}{\lambda M^{2/3}} + \frac{\kappa}{C_i^m \lambda M^{4/3}}\right], \tag{31}$$

where, for for $i = 0, \quad , N$ we denote $C(x_i, t_m)$ by C_i^m and $T(x_i, t_m)$ by T_i^m. This completes the numerical scheme for solving the problem, which now consists simply of (26) and (31).

6 Numerical results

The numerical scheme described above was coded in FORTRAN running a P200 micro under Linux. Before dealing with specific cases, a number of numerical experiments were carried out to check the accuracy and convergence of the numerical scheme. These all confirmed that provided enough mesh points and a small enough time step were used the scheme performed satisfactorily. In each of the cases discussed below, we also performed computations for a number of different time step sizes and mesh point arrangements so that we could be sure that convergence had occurred.

We present a variety of numerical results. In Fig. 2 we consider the de-icing of a layer of ice which has an initial nondimensional thickness of 1/2. For this case we used the values $\theta_i = 100$, $\theta_\infty = \theta_w = -10$, $\theta_f = 0$, $\lambda = 1$, $\Gamma = 20$ and $\kappa = -0.1$. 100 mesh points were used, and we took $\eta_N = 5$, $\phi = 0.3$ and $dt = 0.0001$.

Successive positions of T (solid line) and C (broken line) are shown for $t = 0.0(0.1)0.5$. The behaviour is much as might be expected. The ice layer reduces in thickness near to the rear of the injection slot, but is never completely removed since the wall temperature is less than the freezing temperature. Further downstream, the influence of the cold wing and the

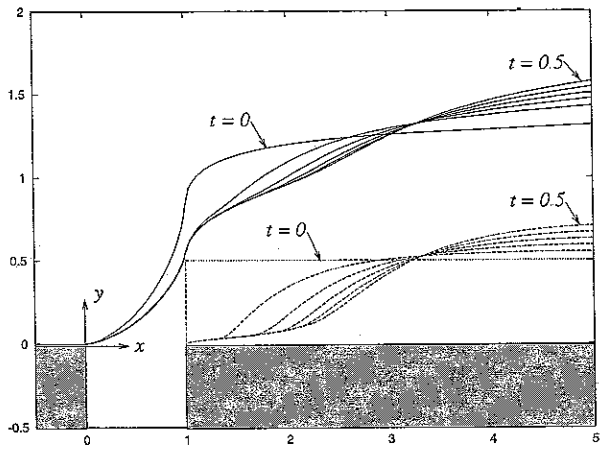

Fig. 2. De-icing for an ice layer of initial thickness 0 5 with an injection temperature of 100 Nondimensional free streamline height T (solid line) and nondimensional ice-layer thickness C (broken line) plotted against nondimensional downstream distance x

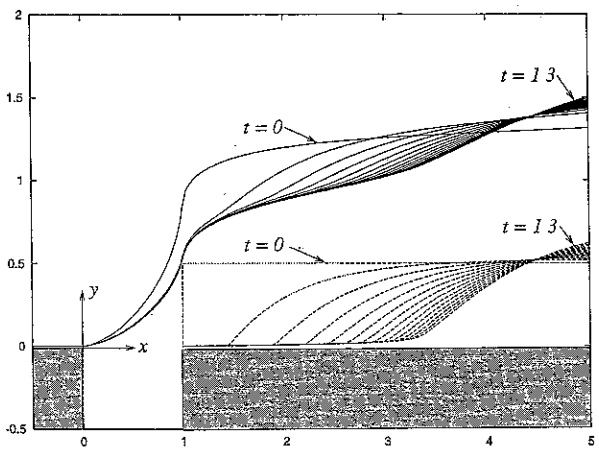

Fig. 3. De-icing for an ice layer of initial thickness 0 5 with an injection temperature of 100 and almost isothermal ice Nondimensional free streamline height T (solid line) and nondimensional ice layer thickness C (broken line) plotted against nondimensional downstream distance x

cold cross flow is felt as the temperature gradient on the ice boundary changes sign and the ice layer begins to grow

In Fig. 3, the parameters are identical to those in Fig. 2, save for the fact that the wall temperature is now chosen to be $\theta_w = -1$ The ice layer is therfore almost isothermal, and it is possible for almost complete melting of the ice layer to take place Results are shown for $t = 0\ 0(0\ 1)1\ 3$; the ice is all but completely removed up to about $x = 3\ 5$ Thereafter the thickness of the ice layer increases as before One way of interpreting Fig. 3 is that it begins to show the approach to the only "steady state" that exists for this formulation of the problem, wherein the ice is completely removed up to the point where the surface temperature gradient of the film changed sign Downstream of this point in this steady state the ice layer is infinitely thick

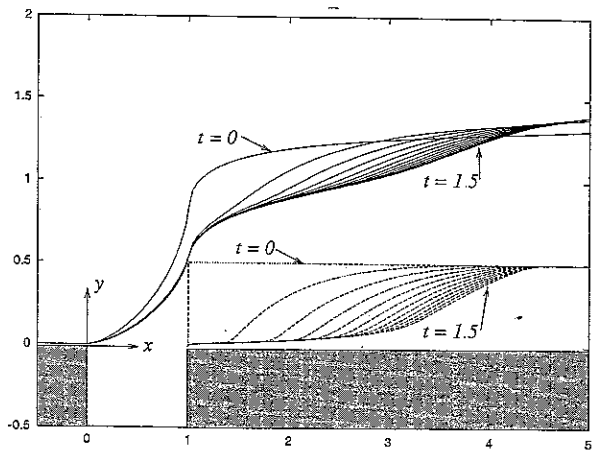

Fig. 4. De-icing for an ice layer of initial thickness 0 5 with no ice growth and an injection temperature of 200. Nondimensional free streamline height T (solid line) and nondimensional ice layer thickness C (broken line) plotted against nondimensional downstream distance x

In the form described above, whenever the cross flow has a temperature below the melting temperature of the ice the model inevitably predicts ice layers that grow as x increases. An additional mechanism of ice formation is also present when the wing temperature is lower than the melting temperature of the ice In reality, of course, the amount of ice that grows depends crucially upon how much water vapour is present in the injected gas One interesting (and possibly more realistic) version of the problem therefore occurs when we assume that no freezable material is present in the cross flow or the film flow (and consequently any ice that melts to become water is "instantly removed").

Figure 4 shows results in a case where no ice growth is permitted Again the layer of ice had an initial nondimensional thickness of 1/2, and we used the values $\theta_i = 200$, $\theta_\infty = \theta_w = -10$, $\theta_f = 0$, $\lambda = 1$, $\Gamma = 20$ and $\kappa = -0.05$ 100 mesh points were used, and we took $\eta_N = 5$, $\phi = 0\ 3$ and $dt = 0\ 0001$ Results are shown for $t = 0\ 0(0\ 1)1\ 5$. Clearly now a nontrivial steady-state solution is attained. The results should also be compared with those in Fig 2 The wall temperatures in the two cases are identical, but in Fig. 4 a higher injection temperature is used The resulting enhanced de-icing effect is evident.

7 Conclusions

We have shown above that it is possible to make detailed predictions of the performance of a slot-injection system for de-icing by using a standard heat transfer and phase change model coupled with incompressible aerodynamics theory One of the potentially valuable results of the theoretical work is the identification of the key nondimensional parameters λ^* and Γ^* and the temperature ratios that control the process.

As suggested above, there are a great deal of amendments and extensions that could be made to the model. These include·

(i) Consideration of a case where the heat transfer to the wing is governed by a Newton cooling type condition In this instance an exact solution of the convection-diffusion equation in Sect. 5 2 is no longer available, and it would be necessary to proceed numerically Once a

von Mises transformation has been used, however, this is a simple matter and need not slow down the numerical scheme excessively

(ii) Consideration of a case where water liberated by the melting of the ice upstream may be redeposited on the ice layer downstream, with consequent refreezing The inclusion of this extra mechanism would require a little extra modelling, but this could easily be incorporated into the numerical scheme

(iii) Using a time-varying pressure in the slot to expel the hot air (This might be useful if it was required to devise a system which could both de-ice and anti-ice without using excess heat by adjusting the mass flow out of the slot.)

It is essential that the development of efficient methods for de-icing aircraft and other structures continues As to the importance of preventing ice from forming on aircraft wings, it is perhaps apposite to conclude with a quotation from R. Kapustin, a former NTSB (National Transportation Safety Bureau) investigator [5]. He remarks:

"Frankly, I don't know how much more often you can tell people that you have to have a clean aeroplane. You can't have ice on it. . I think we need crew members to be aware of the fact that if you load an aeroplane up with ice, you're probably going to die."

Acknowledgement

MPP acknowledges the financial assistance of the EPSRC for a studentship during which the research of this topic was undertaken

References

[1] Shin, J , Berkowitz, B., Chen, H , Cebeci, T · Prediction of ice shapes and their effect on airfoil drag. J. Aircraft **31,** 263–270 (1994)
[2] Kiernan, V : Deicing in the wings. Technol. Rev **98,** 14–15 (1995)
[3] Thomas, S., Cassoni, R., MacArthur, C · Aircraft anti-icing and de-icing techniques and modelling. J. Aircraft **33,** 841–854 (1996).
[4] Kohlmann, D , Schweikhard, W , Evanich, P · Icing-tunnel tests of a glycol-exuding, porous leading-edge ice protection system J Aircraft **19,** 647–654 (1982).
[5] Faith, N.: Black box - The final investigations London: Macmillan 1996
[6] Fitt, A. D , Ockendon, J R., Jones, T V · Aerodynamics of slot film cooling: theory and experiment. J. Fluid. Mech. **160,** 15–27 (1985)
[7] Fitt, A D , Wilmott, P · Slot-film cooling – the effect of separation angle. Acta Mech. **103,** 79–88 (1994)
[8] Fitt, A. D , Stefanidis, V · Film cooling effectiveness for subsonic slot injection into a cross flow Acta Mech **128,** 233–242 (1998)
[9] Cole, J. D , Aroesty, J · The blowhard problem-inviscid flows with surface injection Int J Heat Mass Transfer **11,** 1167–1183 (1968).
[10] Lide, D. R. (Editor-in-Chief): CRC handbook of chemistry and physics, 78th ed. Boca-Raton: CRC Press, 1997

Authors' address: A. D Fitt and M P Pope, Faculty of Mathematical Studies, University of Southampton, Southampton SO17 1BJ, UK